Taylor & Francis
Taylor & Francis Group

ORIGINAL RESEARCH

🔓 OPEN ACCESS   Check for updates

Localization-associated immune phenotypes of clonally expanded tumor-infiltrating T cells and distribution of their target antigens in rectal cancer

Livius Penter [a,b], Kerstin Dietze[a], Julia Ritter[c], Maria Fernanda Lammoglia Cobo [a], Josefin Garmshausen[a,d], Felix Aigner[e], Lars Bullinger[a,d], Holger Hackstein[f], Sandra Wienzek-Lischka[g], Thomas Blankenstein[b,d,h,i], Michael Hummel[c,d], Klaus Dornmair[j], and Leo Hansmann [a,b,d]

[a]Department of Hematology, Oncology, and Tumor Immunology, Charité – Universitätsmedizin Berlin (CVK), Berlin, Germany; [b]Berlin Institute of Health (BIH), Berlin, Germany; [c]Institute for Pathology, Charité – Universitätsmedizin Berlin, Berlin, Germany; [d]German Cancer Consortium (DKTK), Partner site Berlin, Berlin, Germany; [e]Department of Surgery, Charité – Universitätsmedizin Berlin (CCM and CVK), Berlin, Germany; [f]Transfusion Medicine, University Hospital Erlangen, Erlangen, Germany; [g]Institute for Clinical Immunology and Transfusion Medicine, Justus-Liebig-University Giessen, Giessen, Germany; [h]Institute for Immunology Charité – Universitätsmedizin Berlin, Berlin, Germany; [i]Molecular Immunology and Gene Therapy, Max-Delbrück-Center for Molecular Medicine (MDC) Berlin, Berlin, Germany; [j]Institute of Clinical Neuroimmunology, Biomedical Center and Hospital of the LMU, Munich, Germany

ABSTRACT

The degree and type of T cell infiltration influence rectal cancer prognosis regardless of classical tumor staging. We asked whether clonal expansion and tumor infiltration are restricted to selected-phenotype T cells; which clones are accessible in peripheral blood; and what the spatial distribution of their target antigens is.

From five rectal cancer patients, we isolated paired tumor-infiltrating T cells (TILs) and T cells from unaffected rectum mucosa (T_{UM}) using 13-parameter FACS single cell index sorting. TCRαβ sequences, cytokine, and transcription factor expression were determined with single cell sequencing. TILs and T_{UM} occupied distinct phenotype compartments and clonal expansion predominantly occurred within CD8$^+$ T cells. Expanded TIL clones identified by paired TCRαβ sequencing and exclusively detectable in the tumor showed characteristic PD-1 and TIM-3 expression. TCRβ repertoire sequencing identified 49 out of 149 expanded TIL clones circulating in peripheral blood and 41 (84%) of these were PD-1$^-$ TIM-3$^-$. To determine whether clonal expansion of predominantly tumor-infiltrating T cell clones was driven by antigens uniquely presented in tumor tissue, selected TCRs were reconstructed and incubated with cells isolated from corresponding tumor or unaffected mucosa. The majority of clones exclusively detected in the tumor recognized antigen at both sites.

In summary, rectal cancer is infiltrated with expanded distinct-phenotype T cell clones that either i) predominantly infiltrate the tumor, ii) predominantly infiltrate the unaffected mucosa, or iii) overlap between tumor, unaffected mucosa, and peripheral blood. However, the target antigens of predominantly tumor-infiltrating TIL clones do not appear to be restricted to tumor tissue.

Introduction

The incidence of colorectal cancer ranks fourth in men and third in women among all cancer entities and the five year survival rate is approximately 64% for all stages combined.[1] Among a variety of prognostic parameters, the type and density of tumor-infiltrating T cells (TILs) have been shown to affect clinical outcomes and overall survival independent of classical tumor-node-metastasis (TNM) staging.[2–7]

T cell function is determined by T cell receptor (TCR) specificity and the expression patterns of characteristic transcription factors and cytokines.[8–12] Depending on their differentiation state, T cells can contribute to recognition and elimination of (foreign) antigens, autoimmunity, induction of tolerance, and effective B cell responses. T cell-mediated tumor control relies on the integration of antigen-dependent mechanisms (T cell specificity) and mechanisms that are not directly antigen-dependent (immune checkpoints, microenvironment).

According to current understanding, the role of TILs includes the recognition and killing of tumor cells based on their presentation of mutation-derived neo-antigens. In fact, subsets of T cells from colorectal cancer patients have been shown to recognize neo-antigens. Patients with microsatellite instability, who can be expected to harbor high mutational loads, have increased numbers of TILs and better clinical outcomes.[13,14] Furthermore, the therapeutic success of adoptively transferred *in vitro*-expanded neo-antigen-specific T cells highlights their outstanding role in cancer control.[15] In addition to neo-antigens, certain unmutated self-antigens have been shown to induce tumor-directed T cell responses even across different patients.[16]

T cell function is critically dependent on co-stimulatory and co-inhibitory signals. Expression of immune checkpoint molecules (PD-1 and TIM-3 among others) on colorectal cancer-infiltrating T cells suggests an exhausted immune

phenotype interfering with anti-tumor T cell function.[17] However, treatment of colorectal cancer with antibodies against PD-1 or its ligand PD-L1 has not been effective to date except in patients with a high mutational burden.[13,14,18,19]

Defining the functions of different phenotype TILs and the spatial distribution of their target antigens is critical for understanding the composition of immune cells in the cancer-associated microenvironment and for the design of novel immunotherapies. We asked whether clonal expansion and tumor infiltration are restricted to selected phenotype and specificity T cells, and which clones are accessible in the peripheral blood of rectal cancer patients. To minimize phenotype diversity due to location-dependent molecular and clinical features in colorectal cancer,[20,21] we restricted the study to rectal cancer patients. Our technologies for single cell phenotyping and TCR sequencing[22–24] comparatively defined clonal expansion-associated immune phenotypes of T cells from cancer tissue and adjacent unaffected mucosa from five treatment-naïve patients at the single cell level. The identified clones were tracked in the peripheral blood of the same patients at the time of surgical tumor removal and one follow-up visit using multi-parameter flow cytometry, TCRβ repertoire and single cell sequencing.[25] Selected T cell clones were recombinantly expressed[26] and incubated with cells isolated from tumor and unaffected mucosa of the same patients to determine the spatial distribution of the corresponding target antigens (Figure 1 for study specimens and workflow).

Results

Tumor infiltration is associated with characteristic T cell immune phenotypes

Rectal cancer shapes its microenvironment by attracting and re-programming selected types of (immune) cells, supporting tolerance and immune evasion. We hypothesized that immune phenotypes of tumor-infiltrating T cells (TILs) would be substantially different from T cells infiltrating the adjacent unaffected mucosa (T_{UM}).

Multi-parameter flow cytometry (FACS) was used to define T cell immune phenotypes from TILs and T_{UM}, isolated in parallel from surgical specimens of five treatment-naïve rectal cancer patients (Figure 1, Table 1). The FACS panel included 13 markers for the identification of major states of T cell differentiation and selected immune checkpoint molecules (Suppl. Table 1). Using t-stochastic neighbor embedding (t-SNE), we could identify phenotype compartments occupied by i) TILs, ii) T_{UM}, and iii) T cells with phenotype characteristics overlapping between both sites (Figure 2(a)). Although the degree of phenotype overlap varied between individual patients, these three compartments were consistently identified in all patients (Suppl. Figure 1). CD8$^+$ T cell phenotypes were especially distinct between TILs and T_{UM} (Figure 2). While CD38 and PD-1 were expressed on significantly more CD8$^+$ TILs when compared to T_{UM}, B- and T-lymphocyte attenuator (BTLA) was expressed at higher frequencies on CD8$^+$ T_{UM} (Figure 2(b,c)). The immune checkpoint molecule TIM-3, and CD57, a marker associated with exhausted-phenotype T cells, were also enriched on TILs compared to T_{UM}, although this finding did not reach statistical significance.

Clonal expansion predominantly occurs in T cells with distinct immune phenotypes

Previous studies have reported clonal expansion of CD4$^+$ and CD8$^+$ TILs in colorectal cancer.[16,22,27] We asked whether clonal T cell expansion was associated with particular immune phenotypes and applied our technology for single cell paired TCRαβ and phenotype sequencing in combination with 13-parameter FACS index sorting[24] to four selected rectal cancer patients. Randomly selected single TCRαβ$^+$ TILs and T_{UM} were index-sorted for single cell phenotyping and sequencing (Figure 3(a), Suppl. Figures 2 and 3). Clonal expansion was defined as the detection of at least two T cells with identical TCRαβ complementarity-determining region (CDR)-3 amino acid sequences. Numbers of expanded clones were not significantly different between TILs and T_{UM} (Figure 3(b)). Independent of tissue location, expanded T cell clones were predominantly CD8$^+$ (134 of 149 TIL clones and 85 of 105
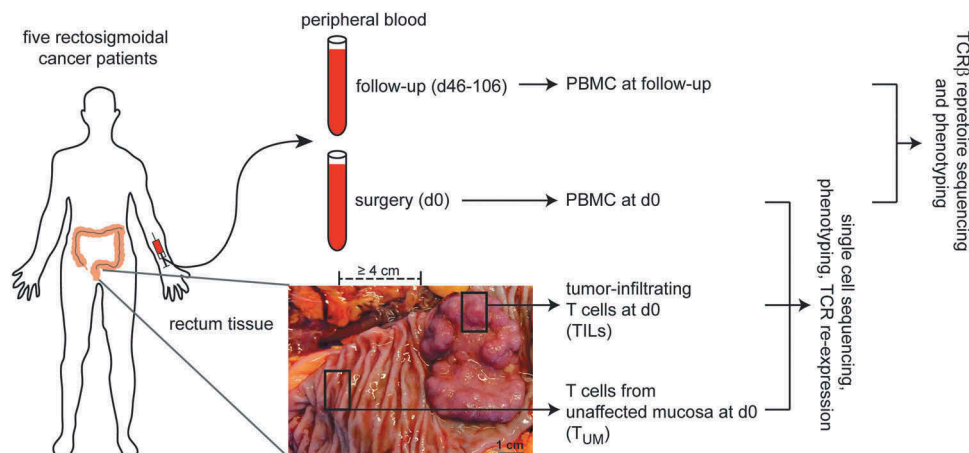

Figure 1. Study specimens and workflow. The distance between the tumor margin and the specimen of unaffected mucosa tissue was > 4 cm for all cases but varied between patients. PBMC: peripheral blood mononuclear cells, TILs: tumor-infiltrating T cells, T_{UM}: T cells from unaffected mucosa, TCR: T cell receptor, d: day after surgery.

Table 1. Patient characteristics.

Pt	Sex	Age (years)	Histology	Tumor stage	MSI	HLA class 1	Clinical follow-up
1	f	80	Moderately differentiated adenocarcinoma	pT3 pN2a (4/12) M0 G2 R0 L0 V0	No	A* 02:01, 11:01 B* 08:01, 15:01 C* 03:04, 07:01	no follow-up data available
2	m	76	Mucinous adenocarcinoma	pT3(m) pN0 (0/14) M0 R0 L0 V0	No	A* 01:01, 68:01 B* 51:01, 52:01 C* 04:01, 12:02	alive +20 months, relapse-free
3	m	57	Moderately differentiated adenocarcinoma	pT3 pN0 (0/13) M0 G2 R0 L0 V0	No	A* 32:01, 33:01 B* 07:05, 40:06 C* 15:02, 15:05	alive +20 months, relapse-free
4	m	62	Moderately differentiated partially mucinous (< 30%) adenocarcinoma	pT2 pN0 (0/16) M0 G2 R0 L0 V0	No	A* 24:02, 26:01 B* 13:02, 18:01 C* 06:02, 07:01	no follow-up data available
5	m	77	Moderately differentiated adenocarcinoma	pT2 pN0 (0/14) M0 G2 R0 L0 V0	No	n.d.	death +1 month due to complication

Pt: patient, f: female, m: male, MSI: microsatellite instability, L0: no lymphatic vessel invasion, V0: no venous invasion, (m): multiple primary tumors in a single site, n. d.: not determined

T_{UM} clones) (Figure 3(c)). Clonally expanded TILs could be distinguished by phenotype from clonally expanded T_{UM} (Figure 3(d), Suppl. Figure 4), as clonally expanded TILs were significantly more frequently CD38+, PD-1+, and TIM-3+ (Figure 3(e)). *IFNG*, *PRF1*, and *GZMB* expression was significantly different between clonally expanded and non-expanded T cells (Suppl. Figure 5) and followed the same patterns in TILs and T_{UM}. Notably, the transcription factor *FOXP3* was predominantly expressed in non-expanded TILs (Figure 3(a,f)).

Selectively tumor-infiltrating T cell clones express the checkpoint molecules TIM-3 and PD-1 and rarely circulate in peripheral blood

We asked whether subsets of clonally expanded TILs were preferentially detectable in the tumor, whether they overlapped with adjacent unaffected mucosa or peripheral blood, and to what extent circulation in peripheral blood was affected by complete tumor removal. Peripheral blood mononuclear cells (PBMCs) were isolated from each patient at the day of surgery and at one follow-up visit (day 46–106 after surgery, Figure 1). Bulk CD8+ and CD8− T cells were FACS-sorted (on average 5.8×10^5 and 1.2×10^6 cells per patient respectively, Suppl. Table 2, Suppl. Fig. 6) and their TCRβ repertoires were sequenced using deep sequencing. As prior experiments had shown that clonal T cell expansion in TILs and T_{UM} predominantly occurred in the CD8+ compartment (Figure 3(c)), we focused on CD8+ peripheral blood T cells for repertoire sequencing.

We detected on average 962 (range 343–2,244) individual CD8+ T cell clones per time point and patient by peripheral blood TCRβ repertoire sequencing (Suppl. Table 2). TCR sequences from single TILs, T_{UM}, and the corresponding peripheral blood showed substantial clonal overlap within individual patients but not a single TCR overlapped between different patients (Figure 4(a)). From a total of 149 expanded TIL clones, 29 (19.5%) were detectable in the unaffected mucosa and 49 (32.9%) in the peripheral blood, whereas 92 (61.7 %) were exclusively detectable among TILs (Figure 4(a,b)). Predominantly tumor-infiltrating clones expressed PD-1 and TIM-3 (42.6% and 21.2% of the clones respectively), whereas TIL clones that overlapped with unaffected mucosa and/or peripheral blood were PD-1− TIM-3− (Figure 4(c)). When focusing on the TIL clones

detectable in the peripheral blood, PD-1 and TIM-3 expression was mostly absent (84% of the clones, Figure 4(d)).

The accurate determination of clonal overlap between TILs and T_{UM} relies on the stability of immune phenotypes over time and the detection limit of our sequencing assays.

The immune phenotypes of peripheral blood CD8+ T cells, in particular CD38, integrin beta-7, and CD45RA expression, were substantially different from TILs (Figure 4(e)), albeit stable over time as shown for CD4 and CD45RA as examples (Figure 4(f)). PD-1 and TIM-3 expression was enriched on clones selectively infiltrating the tumor (Figure 4(c)) and rare in peripheral blood (<1.4% and <6.6% of CD8+ T cells for PD-1 and TIM-3, respectively, Figure 4(e)). To focus on these rare populations, we specifically sorted single peripheral blood T cells with increased PD-1 or TIM-3 expression (184 cells per population and patient, Suppl. Fig. 7) and sequenced their TCRs using single cell sequencing (Suppl. Tab. 3). Clones were determined to be absent in the peripheral blood if they could not be detected by TCRβ repertoire or single cell sequencing (Figure 4(a,b)). The dominantly expanded CD8+ T cell clones in the peripheral blood were stable across different time points and clones with a frequency of >0.2% in peripheral blood at the day of surgery (day 0) were consistently detectable in the follow-up samples (Figure 4(g)) regardless of surgical tumor removal. This suggests that cues other than tumor neo-antigens are likely to be the drivers of their expansion.

Expanded T cell clones, irrespective of their origins, recognize antigens present in corresponding tumor and unaffected mucosa tissues

PD-1+ TIM-3+ expanded T cell clones predominantly infiltrated the tumor. We asked whether the presentation of antigens driving clonal expansion of predominantly tumor-infiltrating T cells was restricted to tumor tissue.

Based on their frequencies, we chose four T cell clones exclusively detected in the tumor and three clones overlapping between tumor, unaffected mucosa, and peripheral blood (Figure 5(a), Table 2). Their TCRs were reconstructed and functionally expressed on 58α− β− T hybridoma cells that had previously been transfected with GFP under the control of nuclear factor of activated T cells (NFAT)[26] and human CD8αβ chains.[28] GFP expression and mouse IL-2
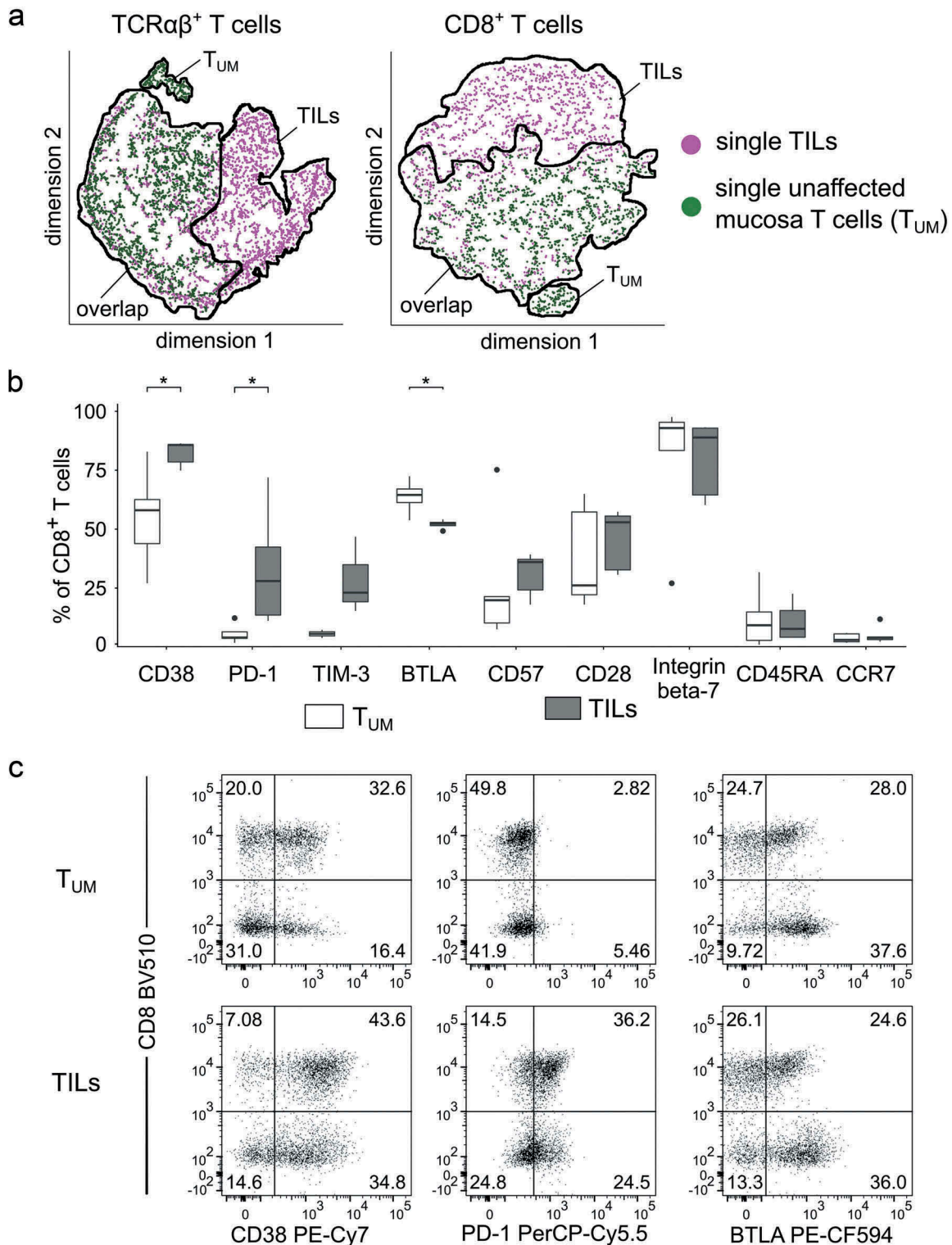
Figure 2. Subsets of TILs and T_{UM} show distinct immune phenotypes. TILs and T_{UM} pairs from five patients were stained in parallel with a multi-parameter FACS panel. (a) t-SNE visualization distinguished TILs from T_{UM} and identified immune phenotype compartments i) predominantly occupied by TILs, ii) predominantly occupied by T_{UM}, or iii) occupied by T cells from both locations. Each data point represents one single cell from patient 3 as an example. (b) Detailed immune phenotypes of CD8$^+$ TILs and CD8$^+$ T_{UM} from all n = 5 patients (n = 3 for TIM-3, n = 4 for CD28 and BTLA) determined by FACS were visualized as box plots. * p < 0.05, Student's t-test (c) shows detailed FACS plots for the parameters significantly differently expressed between TILs and T_{UM} from patient 3 as an example. Gates for CD38 and BTLA were set based on expression of the respective markers on TCRαβ$^-$ cells. PD-1 gates were adjusted to the 98th expression percentile on TCRαβ$^-$ cells. All FACS plots were pre-gated on single live TCRαβ$^+$ lymphocytes.

production were detected as readouts for antigen-dependent T cell activation. After stimulation with plate-bound anti-mouse CD3 (positive control), the seven 58α$^-$β$^-$ cell lines expressing recombinant TCRs were on average 77% GFP$^+$ and produced on average 8,613 pg/ml murine IL-2 (Suppl. Fig. 8). To test whether target antigens were presented, TCR-recombinant 58α$^-$β$^-$ cells were co-incubated with left-over cells isolated from tumor and unaffected mucosa
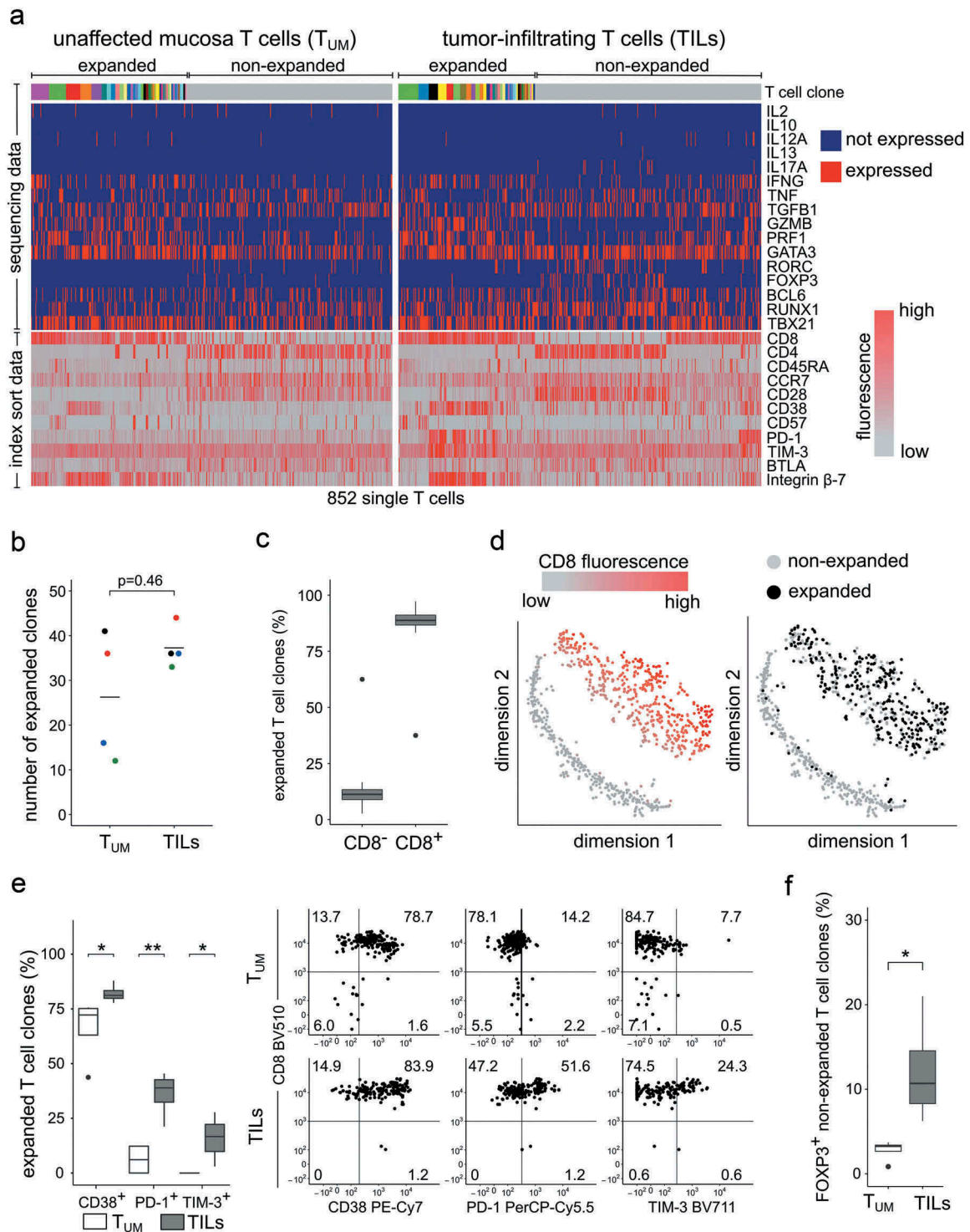
Figure 3. Clonal expansion-associated phenotype patterns of TILs and T$_{UM}$. (a) Parallel next generation sequencing of TCRαβ, transcription factor, and cytokine genes from amplified cDNA of single TILs and T$_{UM}$ (Suppl. Figure 2 for sorting gates). The sequencing and FACS data of single cells are arranged in columns with each column representing one single cell. The top bar indicates TCR sequences; adjacent columns with the same color in the top bar indicate single cells with identical CDR3 amino acid sequences of their TCRαβ genes. Clonal expansion was defined as the detection of at least two cells with identical TCRαβ sequences. The lower part of the heatmap is derived from the corresponding FACS index sort data and fluorescence intensities are color-coded from grey (lowest expression) to red (highest expression) for the indicated parameters. The heatmap shows data from patient 1 as an example (see Suppl. Figure 3 for detailed data of all patients in the study). (b) shows numbers of expanded T cell clones per patient. Each data point represents one patient (black, blue, red, green for patients 1, 2, 3, 4, respectively). (c) shows CD8 expression on expanded T cell clones. (d) Single TCR-sequenced TILs and T$_{UM}$ from patient 1 as an example are visualized with t-SNE. Clonal expansion was enriched in CD8$^+$ compartments. (e) shows selected markers significantly differentially expressed between clonally expanded TILs and T$_{UM}$. The left panel shows data from all patients summarized as box plots. Each data point in the FACS plots (data from patient 1 as an example) represents one single cell belonging to an expanded T cell clone. An individual clone was considered positive for a particular marker based on the majority of cells of the respective clone. Gates for CD38 were set based on expression on TCRαβ$^-$ cells. TIM-3 and PD-1 gates were adjusted to the 98th expression percentile on TCRαβ$^-$ cells. (f) shows *FOXP3* expression determined by sequencing in non-expanded T cell clones. Box plots: The lower and upper hinges correspond to the 25th and 75th percentiles. The upper and lower whiskers extend from the hinge to the largest or lowest values respectively, no further than 1.5 x inter-quartile range. Data beyond the end of the whiskers are plotted individually.
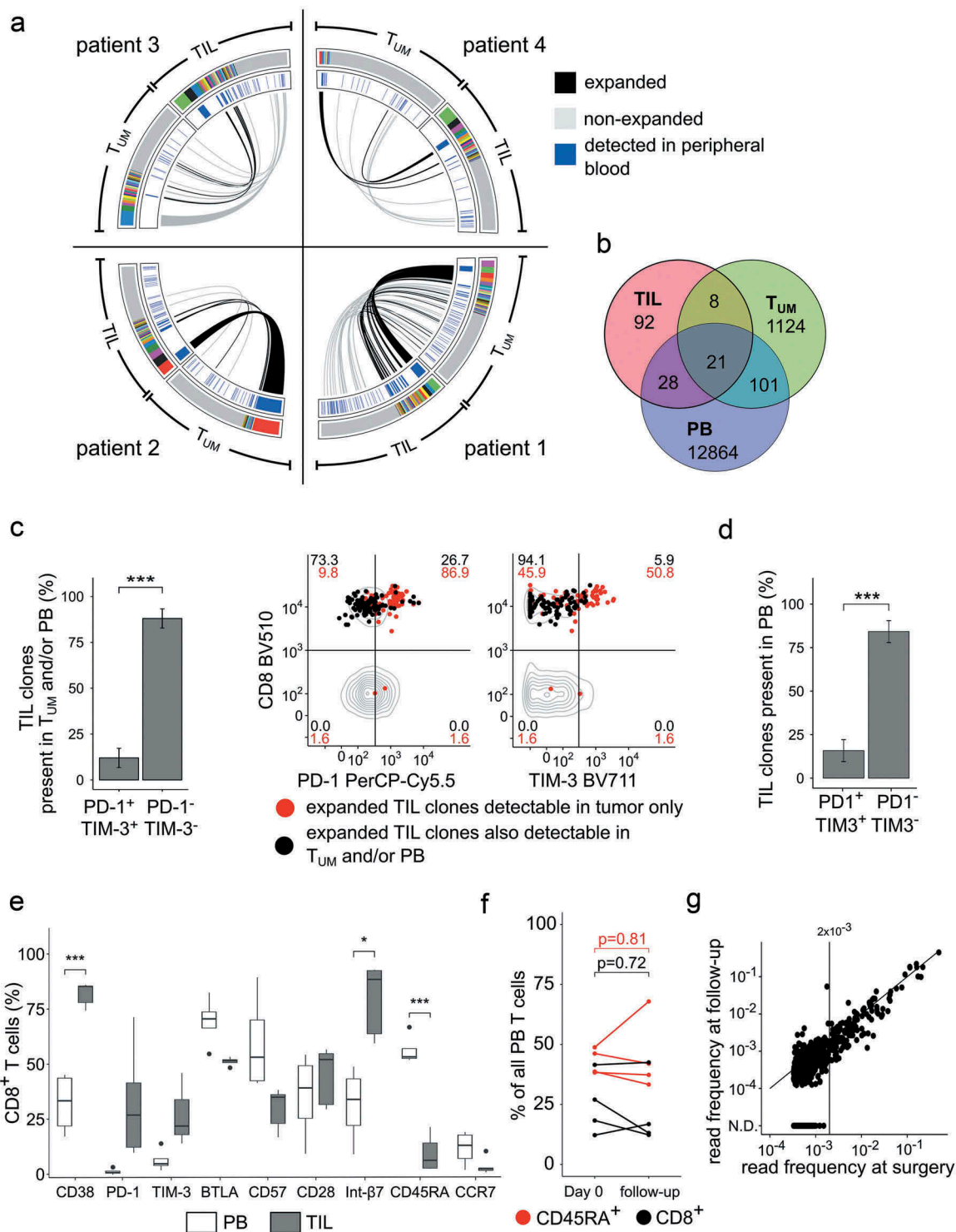
*p < 0.05, **p < 0.01, Student's t-test

Figure 4. Clonal overlap between TILs and T_{UM} is associated with characteristic immune phenotypes. The outer circle shows single cell TCRαβ sequencing data of TILs and T_{UM} from patients 1–4. Cells with the same TCRβ CDR3 sequences are represented with the same color and cells are ordered by clone size. Grey represents single non-expanded T cells. The inner circle indicates whether a particular T cell clone was detected in peripheral blood by TCRβ repertoire or single cell sequencing at any time point. Connectors indicate clonal overlap between TILs and T_{UM} (black if the clone was expanded within TILs, otherwise grey). (b) Absolute numbers of overlapping clones between clonally expanded TILs, T_{UM} (clonally expanded and non-expanded), and peripheral blood are shown in a Venn diagram for patients 1–4 combined. (c) The left panel shows the frequency of PD-1 and/or TIM-3 expression on expanded TIL clones also detectable in peripheral blood and/or unaffected mucosa for all patients combined. PD-1$^+$ TIM-3$^+$ summarizes cells that were PD-1$^+$ and/or TIM-3$^+$. PD-1$^-$ TIM-3$^-$ cells were negative for both markers. FACS plots show data from patient 1 as an example. Each data point represents one single cell of an expanded T cell clone. An individual clone was considered positive for a particular marker based on the majority of cells of the respective clone. PD-1 and TIM-3 gates were adjusted to the 98th expression percentile on TCRαβ$^-$ cells. (d) shows the frequencies of PD-1 and/or TIM-3 expression on expanded TIL clones detectable in peripheral blood for all patients combined. PD-1$^+$ TIM-3$^+$ summarizes cells that were PD-1$^+$ and/or TIM-3$^+$. PD-1$^-$ TIM-3$^-$ cells were negative for both markers. (e) Paired TIL and peripheral blood FACS phenotype data are visualized as box plots. The lower and upper hinges correspond to the 25th and 75th percentiles. The upper and lower whiskers extend from the hinge to the largest or lowest values respectively, no further than 1.5 x inter-quartile range. Data beyond the end of the whiskers are plotted individually. TIL data are derived from all n = 5 patients (n = 3 for TIM-3, n = 4 for CD28 and BTLA) including n = 4 patients for peripheral blood phenotypes. (f) illustrates the consistency of peripheral blood immune phenotypes over time. (g) shows frequencies of CD8$^+$ peripheral blood T cell clones determined with TCRβ repertoire sequencing at the day of surgery (d0) and follow-up. The figure shows the most expanded clones covering 80% of all sequencing reads per patient and time point. Each data point represents one out of 519 clones from all patients combined.
PB: peripheral blood; * p < 0.05, ** p < 0.01, *** p < 0.005, Student's t-test
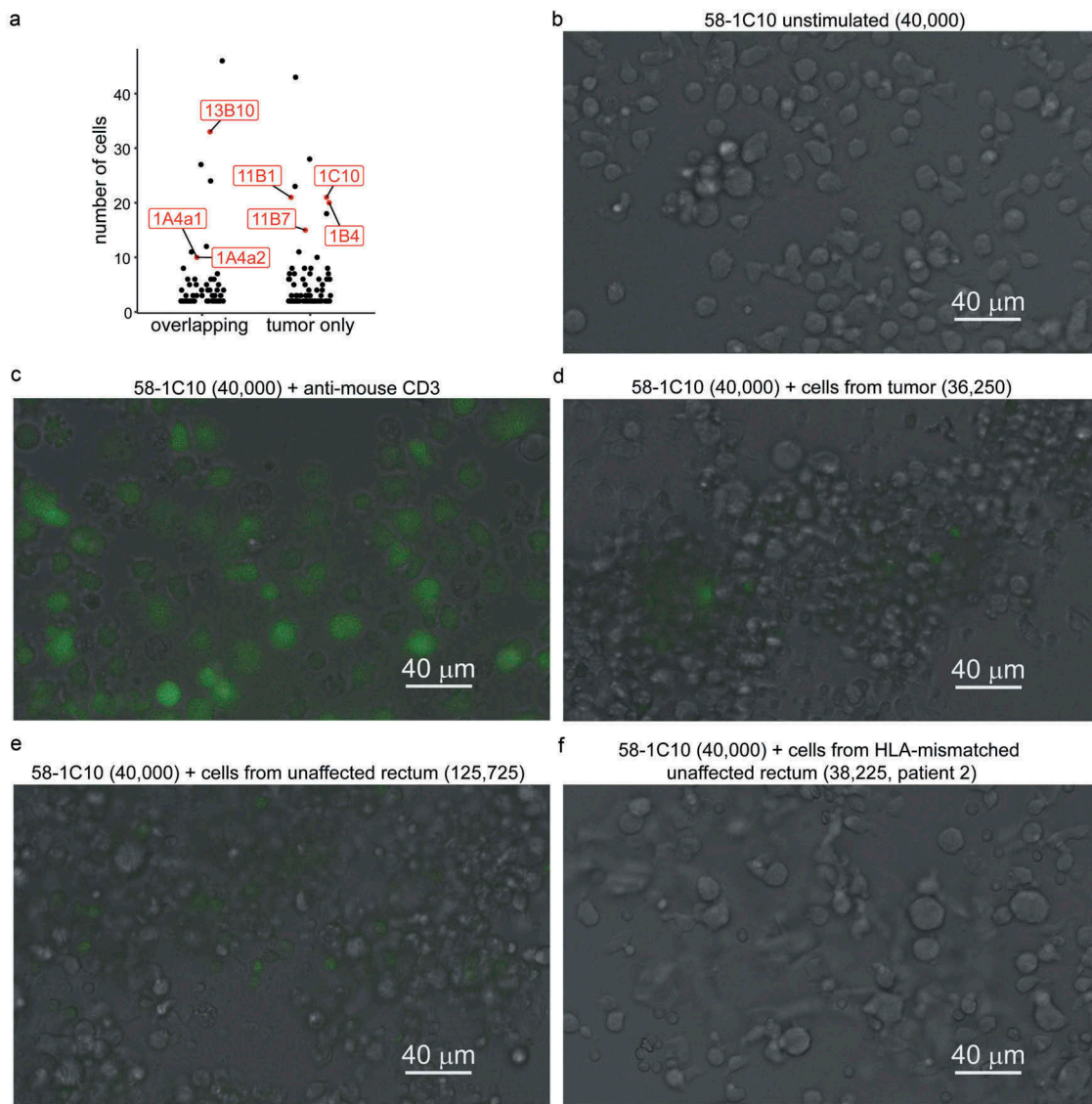
Figure 5. Spatial presentation of target antigens of predominantly tumor-infiltrating expanded T cells. (a) shows the expansion of individual T cell clones only detectable in the tumor or overlapping between tumor, unaffected mucosa, and peripheral blood. The figure shows data from all four patients combined and each data point represents one clone. Clones selected for reconstruction and expression in 58α⁻β⁻ cell lines were highlighted in red. CDR3 sequences and corresponding patients for each reconstructed clone can be found in Table 2. (b–f) shows fluorescence microscopy of 58-1C10 (as an example for an expanded TCR only detectable in TILs) unstimulated, stimulated with plate-bound anti-mouse CD3 (positive control), or after co-incubation with cells from the corresponding tumor, unaffected mucosa tissue, or HLA-mismatched unaffected mucosa (negative control). Numbers in parentheses indicate absolute cell numbers for co-incubation. Fluorescence microscopy was used to screen the entire co-incubation wells for GFP⁺ cells. (d–f) represent images of single GFP⁺ cells if any were detectable in the entire well. See Supplementary Figure 10 for data from all re-expressed TCRs. For detailed cell numbers and culture conditions, see Supplementary Table 4.

Table 2. Spatial distribution and CDR3 amino acid sequences of T cell clones for re-expression on 58α⁻β⁻ cells.

									Detected in		
TCR label	Pt	TRAV	CDR3 alpha amino acid sequence	TRAJ	TRBV	CDR3 beta amino acid sequence	TRBJ	TIL	T_UM	PB
13B10	2	27*01	CAGGVNNNAGNMLTF	39*01	20–1*01	CSARDLRSTDTQYF	2–3*01	Yes	Yes	Yes
11B1	2	8–2*01	CAVSDVSGGYQKVTF	13*02	2*01	CASSGGRASGSGEQFF	2–1*01	Yes	No	No
11B7	2	39*01	CAAPIMEYGNKLVF	47*01	10–2*01	CASTPGLREKLFF	1–4*01	Yes	No	No
1C10	3	21*01	CAVTFPNAGNMLTF	39*01	6–6*01	CASSYGARLNTEAFF	1–1*01	Yes	No	No
1B4	4	13–1*01	CAVTGTASKLTF	44*01	29–1*01	CSVVGQDYEQYF	2–7*01	Yes	No	No
1A4-1	4	19*01	CALSEYGGSQGNLIF	42*01	6–1*01	CASSEASGSWTGELFF	2–2*01	Yes	Yes	Yes
1A4-2	4	1–2*01	CAVTDSNYQLIW	33*01	6–1*01	CASSEASGSWTGELFF	2–2*01	Yes	Yes	Yes

Pt: patient. PB: peripheral blood. TRAV: TCRα V-gene and allele. TRAJ: TCRα J-gene and allele. TRBV: TCRβ V-gene and allele. TRBJ: TCRβ J-gene and allele. TCR-recombinant 58α⁻β⁻ cell lines were named "58-TCR label", e.g. "58-1C10".

tissues (Suppl. Tab. 4 for cell numbers). We detected neither IL-2 production with ELISA nor GFP expression with FACS significantly above background for any TCR-recombinant cell line (Suppl. Fig. 9 as an example). However, by screening with fluorescence microscopy, we could observe single cell aggregates containing GFP⁺ cells that could not be

detected with FACS due to their low frequencies (Figure 5 (b–f)). Of the four expanded TCRs exclusively detected in tumor tissue (Figure 5(a)), one recognized antigen only within cells isolated from the tumor (11B7), one recognized antigen only within cells isolated from unaffected mucosa (1B4), and two got activated by cells from both tumor and unaffected mucosa (1C10 and 11B1, Figure 5(d,e) as an example, Suppl. Fig. 10A for all re-expressed TCRs). From the three expanded TCRs detectable in tumor, unaffected mucosa, and peripheral blood, two were activated by cells isolated from both tumor and unaffected mucosa (13B10, 1A4-1), and one got activated only by cells isolated from unaffected mucosa (1A4-2, Suppl. Fig. 10B).

In conclusion, rectal cancer is infiltrated by expanded T cell clones that either i) selectively infiltrate the tumor but are functionally inhibited by the expression of immune check-point molecules or ii) overlap between tumor, unaffected mucosa, and peripheral blood, show distinct immune pheno-types, and, at least the dominant clones, persist after surgical tumor removal. The antigens underlying selective TIL expan-sion do not appear to be exclusively presented in tumor tissue.

Discussion

A variety of cellular cancer treatment approaches including adop-tive T cell transfer, chimeric antigen receptor (CAR) T cells, immune checkpoint blockade, and bispecific antibodies depend on efficient, targeted T cell functions. We addressed the following questions at the single cell level: i) Which are the phenotypes and presumed functional capacities of rectal cancer-infiltrating T cells, ii) are particular immune phenotypes associated with predomi-nant tumor infiltration, iii) which TIL clones are accessible in peripheral blood, and iv) what is the spatial distribution of target antigens of expanded TIL clones?

Data on detailed immune phenotypes of paired TILs and T_{UM} from the same patients are limited[5] and often disregard the exact location of the tumor (different parts of the colon vs. rectum). Studies addressing clonal T cell interrelatedness at the single cell level are limited to single cases.[16,22,29]

Irrespective of clonal expansion, we identified tumor infiltra-tion-associated T cell immune phenotypes. CD38$^+$ and PD-1$^+$ T cells were significantly enriched among TILs and we observed similar trends for TIM-3 and CD57, though they did not reach statistical significance. PD-1 and TIM-3 have previously been shown to be expressed on colorectal cancer-infiltrating T cells,[17,30] however, PD-1-targeting therapies were particularly effective in tumors with DNA mismatch-repair deficiencies.[31] Notably, none of the patients in our study showed features of microsatellite instability (Table 1). The role of BTLA, a receptor involved in regulation of T cell function, has been under debate. Depending on downstream signaling pathways, BTLA may trans-mit stimulatory or inhibitory signals possibly accounting for its controversial roles in malignant melanoma, gastric, and gall blad-der cancer.[32–37] We show that BTLA was expressed on more than 50% of CD8$^+$ T cells isolated from peripheral blood, tumor, and unaffected mucosa although expression was less on TILs com-pared to T_{UM}. The functional and clinical significance of BTLA expression on TILs and T_{UM} in rectal cancer has to be determined in future studies. Data on CD38 and CD57 expression on TILs in comparison with T_{UM} are limited but CD38 expression has been shown to be induced by the tumor microenvironment and can inhibit CD8$^+$ T cell function via adenosine receptor signaling.[38] Elevated numbers of CD57$^+$ T and NK cells have been reported at the invasive margins of colorectal cancer.[3]

Independent from the particular set of markers, which will be subject to change depending on the selection of parameters and sample size in future studies, we conclude that immune phenotypes of TILs and T_{UM} are substantially different.

Immune phenotypes and functions associated with clonal T cell expansion can only be reliably studied at the single cell level. To complement single cell paired TCRαβ sequencing, additional TCRβ repertoire sequencing was chosen for selected research questions. Tissue samples, especially from tumors and unaffected mucosa, were limited and we were particularly interested in clonal expansion-associated immune phenotypes. Therefore, we applied single cell sequencing, which is superior in terms of efficiency and the parallel determination of single cell immune phenotypes. Surprisingly, numbers of expanded clones were not significantly different between TILs and T_{UM}. While clonal TIL expansion could be tumor-specific/associated, we assume the cues driving clonal T_{UM} expansion not to be directly tumor-related. This assumption is based on the major-ity of expanded T_{UM} clones not being detectable among TILs, but a substantial amount overlapping with peripheral blood and showing phenotype characteristics of functional, non-exhausted T cells (PD-1$^-$ TIM-3$^-$).

In sequencing several hundred single T cells per patient and tissue type, there remains a chance of falsely determining clones to be non-overlapping or non-expanded. However, the identi-fied immune phenotypes were significantly associated with the assigned status (overlapping vs. non-overlapping). In summary, combined single cell flow cytometry and sequencing data suggest the functional differentiation of clonally expanded TILs towards tolerance in an antigen-specific fashion by the expression of immune checkpoint and inhibitory molecules (PD-1, CD57, CD38). *FOXP3* expression in non-expanded TILs can be assumed to support the tolerogenic microenvironment. Albeit not clonally expanded, a substantial proportion of CD4$^+$ TILs were CD45RA$^-$CCR7$^+$CD28$^+$ (Figure 3) characterizing them as central memory T cells.[39,40] Their partial expression of *TGFB* and *FOXP3* mostly in the absence of *PRF1, GZMB*, and *IFNG* suggests tolerogenic differentiation. The clinical significance and underlying differentiation mechanisms of these cells have to be determined in future studies.

It is important to accurately identify TIL clones circulating in the peripheral blood, as a variety of therapeutic approaches rely on the accessibility of tumor-specific T cells in the peripheral blood. Consistent with previous studies,[41] expanded T cell clones in peripheral blood remained mostly stable over time and unchanged months after tumor resection, suggesting that their expansion was not driven by resected tumor-associated neo-antigens. Dominant T cell clones in the peripheral blood of healthy individuals have been considered specific for antigens of chronic infections such as cytomegalovirus (CMV) or Epstein-Barr virus (EBV), among others. In fact, one of the most expanded peripheral blood TCRs in patient 1 (TCRβ CDR3 amino acid sequence: CASSSANYGYTF), which was also expanded among this patient's TILs and T_{UM}, has already been reported CMV-specific.[42]

As previously reported,[17] particular phenotypes enriched in TILs (PD-1^{+}, TIM-3^{+}) were rare in peripheral blood (Figure 4(d)), however, especially PD-1^{+} peripheral blood T cells have previously been considered tumor-specific.[15] To increase the chance of detection, we extended our bulk sequencing data with high-efficiency single cell TCRαβ sequencing of specifically sorted T cell populations with increased PD-1 and TIM-3 expression.

A recent study suggests the distinction of exhausted-phenotype, presumably tumor-specific, T cells and bystander T cells in colorectal and lung cancer based on the expression of the ecto-ATP/ADPase CD39.[43] Selectively rectal cancer-infiltrating T cells were exhausted and functionally inhibited, as represented by PD-1, TIM-3, CD38, and CD57 expression. By re-expressing selected TCRs in 58α⁻β⁻ T hybridoma cell lines and incubating them with cells isolated from their corresponding tissues, we showed that exhausted T cell clones selectively expanded in tumor tissue could recognize antigens presented on cells isolated from either site. The critical antigens appeared to be presented on very few cells close to the detection limit of our assays, which is not surprising since the cell preparations were not enriched for any particular cell type. Supplementary Figure 2 and microscopy (Figure 5) show the majority of cells isolated from rectum tissue were non-lymphocytes. In case a reconstructed TCR did not get activated upon co-incubation, we cannot conclude whether the lack of target antigen was due to the low frequency of antigen-presenting cells or the target antigen indeed not being presented in the investigated tissue. However, in vivo, particular expanded T cell clones selectively infiltrated the tumor tissue and were below the detection limits of our technologies at any other site, including peripheral blood. A variety of mechanisms, such as chemo-attraction, selective antigen accessibility in vivo, or inhibition of T cell expansion by microenvironment-derived cues, among others, could account for this observation. Recent studies on a variety of solid cancers suggest antigens other than neo-antigens to drive clonal TIL expansion in the tumor environment,[16,43,44] which is in support of our findings. The clinical significance of different phenotype TILs preferentially infiltrating tumor tissue has to be determined along with TCR specificities in future cohorts.

In conclusion, rectal cancer is infiltrated by clonally expanded unique-specificity T cells that show dysfunctional/exhausted immune phenotype patterns and rarely circulate in the peripheral blood. Their target antigens, however, do not seem to be exclusively presented in tumor tissue.

Patients and methods/materials and methods

Patients and sample preparation

Surgical specimens (one piece of rectal tumor and one piece of unaffected recto-sigmoidal mucosa per patient) and heparin-anticoagulated peripheral blood at surgery and one follow-up time point were obtained from five treatment-naïve rectal cancer patients. All patients gave written informed consent and the study was approved by the local ethics committee (protocol EA1/007/16 to L.H.). TILs and T_{UM} were isolated from fresh specimens immediately after surgery as previously described.[22] In short,

tissue was cut into small pieces (2–4 mm³) and incubated in PBS containing 10 mM Ethylendiaminetetraacetic acid (EDTA, Invitrogen) for 30 min. Cells in suspension were passed through a 100 μm cell strainer (Corning), tissue was incubated in RPMI1640 containing 5% fetal bovine serum (FBS) and 0.5 mg/ml collagenase (Serva, Collagenase NB 4) for 30 min. Finally, cells were enriched through Percoll (GE Healthcare) gradient centrifugation and cryopreserved. Distances between the tumor and unaffected mucosa specimens varied between patients but unaffected mucosa samples were taken at least 4 cm apart from the macroscopic tumor margin (Figure 1). PBMCs were isolated with Ficoll-Paque PLUS (GE Healthcare) density gradient centrifugation. All cell preparations were cryopreserved in RPMI1640 containing 50% FBS, 10% DMSO before further processing.

Fluorescence-activated cell sorting

Cells were thawed and stained with multicolor panels (Suppl. Table 1). Antibodies were used according to the manufacturer's instructions. TILs and T_{UM} samples from each patient were processed in parallel to minimize instrument and staining variability. For single cell sequencing, single cells were index-sorted directly into 96-well plates pre-filled with OneStep RT-PCR buffer (Qiagen) as previously described.[24] For TCRβ repertoire sequencing, bulk cells were FACS-sorted into tubes prefilled with RPMI1640 containing 2% FBS. DNA was isolated immediately after sorting using the DNeasy Blood & Tissue Kit (Qiagen) and stored at 4°C until further processing. All cells were sorted using a FACSAria™ Fusion high-speed cell sorter (BD Biosciences) equipped with a 70 μm nozzle.

Single cell sequencing and phenotyping

PCR amplification, library preparation, and MiSeq (Illumina) sequencing were done as previously described.[22,24] Sequencing data were processed as previously described[24] and scripts can be downloaded from https://github.com/HansmannLab/TRECA. Cytokines and transcription factors were determined expressed in single cells if we detected more than 10 reads for the respective cytokine or transcription factor transcript.[22] In case of the seven TCRs chosen for re-expression (Figure 5), transcripts of the second TCRα chain of TCR 1A4 were identified by manually screening the sequencing output. No additional TCRα chains could be identified for the remaining six re-expressed TCRs (Table 2).

Clonal expansion was defined as the detection of at least two cells with identical TCRα and TCRβ amino acid sequences. Index sorting assigned exact immune phenotypes to every single sorted cell. Notably, some expanded clones showed heterogeneous marker expression and a clone was considered positive for a particular marker based on the majority (> 50%) of cells with a particular TCR sequence.

TCRβ repertoire sequencing

TCRβ repertoire sequencing was done as previously described and the read frequency cutoff for the definition of individual clones was chosen at 10^{-4}.[25]

Recombinant T cell receptor expression in 58α⁻β⁻ cell lines and co-incubation with tumor and unaffected mucosa cell preparations

Selected TCRs were reconstructed by completing the missing leader, V, and constant region parts with sequences downloaded from IMGT,[45] and expressed in 58α⁻β⁻ cell lines as previously described.[26] 58α⁻β⁻ cell lines also expressed human CD8αβ chains[28] and GFP under the control of nuclear factor of activated T cells (NFAT),[26] so they light up green upon activation. TCR-expression was confirmed by CD3 detection with FACS. As positive controls, TCR-recombinant cell lines were stimulated with plate-bound anti-mouse CD3 in 96-well plates for 16 h. IL-2 was measured in cell culture supernatants using the IL-2 Mouse Uncoated ELISA Kit (Thermo Fisher) and GFP expression was detected with FACS and fluorescence microscopy. For co-incubation experiments (Figure 5 and Suppl. Figs. 9–10), TCR-recombinant 58α⁻β⁻ cells were incubated with cells isolated from i) corresponding tumor, ii) corresponding unaffected mucosa tissue, or iii) tumor or unaffected mucosa from an HLA-mismatched patient as negative control. For TCRs, corresponding patients, and exact co-incubation cell numbers, see Table 2 and Supplementary Table 4. Numbers of cells isolated from tumor or unaffected mucosa tissues varied between patients due to the size of surgical specimens. The majority of cells isolated from tissues were non-lymphocytes (Suppl. Figure 2). All remaining cells from each patient were used for co-incubation experiments (Figure 5, Suppl. Figs. 9 + 10) to maximize the chance of detection of TCR targets in the available specimens. Co-incubations were done in 96-well plates in a volume of 150 μl RPMI1640 containing 10% FBS for 16 h at 37°C and 5% CO₂.

Fluorescence microscopy

Bright field and GFP fluorescence images were recorded separately using a Biorevo BZ-9000E instrument (Keyence) equipped with an S Plan Fluor ELWD 20x lens and overlaid for visualization.

HLA-typing

Genomic DNA samples were amplified using GoTaq Long Range Polymerase (Promega) and HLA-locus-specific primers (NGSgo workflow, GenDx). Pooling of amplicons, fragmentation, adapter ligation, DNA clean-up, indexing PCR, second clean-up, size selection, library pooling, quantification, and denaturation were performed according to the manufacturer's instructions. Sequencing was done on a MiSeq instrument (Illumina) using 300 cycle kits (151 base pairs, paired-end sequencing). Data were analyzed with NGSengine software (GenDx).

Data accessibility

Single cell sequencing data have been made publicly available (DDBJ/EMBL/GenBank accession KCPL00000000, first version KCPL01000000). TCRβ repertoire sequencing data are available online (suppl_online_table_1.xlsx). Single cell cytokine and transcription factor sequencing data along with the corresponding FACS index sort data are available online (suppl_online_table_2.xls).

Disclosure of Potential Conflicts of Interest

No potential conflicts of interest were disclosed

ORCID

Livius Penter 🕮 http://orcid.org/0000-0002-9060-0207
Maria Fernanda Lammoglia Cobo 🕮 http://orcid.org/0000-0002-0369-0364
Leo Hansmann 🕮 http://orcid.org/0000-0003-3790-0128

References

1. Howlader N, Noone AM, Krapcho M, Garshell J, Neyman N, Altekruse SF, Kosary CL, Yu M, Ruhl J, Tatalovich Z, et al. SEER cancer statistics review, 1975-2010. National Cancer Institute. Bethesda, MD, https://seer.cancer.gov/archive/csr/1975_2010/, based on November 2012 SEER data submission, posted to the SEER web site, April 2013.
2. Anitei MG, Zeitoun G, Mlecnik B, Marliot F, Haicheur N, Todosi AM, Kirilovsky A, Lagorce C, Bindea G, Ferariu D, et al. Prognostic and predictive values of the immunoscore in patients with rectal cancer. Clin Cancer Res. 2014;20:1891–1899. doi:10.1158/1078-0432.CCR-13-2830.
3. Bindea G, Mlecnik B, Tosolini M, Kirilovsky A, Waldner M, Obenauf AC, Angell H, Fredriksen T, Lafontaine L, Berger A, et al. Spatiotemporal dynamics of intratumoral immune cells reveal the immune landscape in human cancer. Immunity. 2013;39:782–795. doi:10.1016/j.immuni.2013.10.003.
4. Fridman WH, Pages F, Sautes-Fridman C, Galon J. The immune contexture in human tumours: impact on clinical outcome. Nat Rev Cancer. 2012;12:298–306. doi:10.1038/nrc3245.
5. Galon J, Costes A, Sanchez-Cabo F, Kirilovsky A, Mlecnik B, Lagorce-Pages C, Tosolini M, Camus M, Berger A, Wind P, et al. Type, density, and location of immune cells within human colorectal tumors predict clinical outcome. Science. 2006;313:1960–1964. doi:10.1126/science.1129139.
6. Mlecnik B, Bindea G, Angell HK, Maby P, Angelova M, Tougeron D, Church SE, Lafontaine L, Fischer M, Fredriksen T, et al. Integrative analyses of colorectal cancer show immunoscore is a stronger predictor of patient survival than microsatellite

instability. Immunity. 2016;44:698–711. doi:10.1016/j.immuni.2016.02.025.

7. Pages F, Berger A, Camus M, Sanchez-Cabo F, Costes A, Molidor R, Mlecnik B, Kirilovsky A, Nilsson M, Damotte D, et al. Effector memory T cells, early metastasis, and survival in colorectal cancer. N Engl J Med. 2005;353:2654–2666. doi:10.1056/NEJMoa051424.

8. Davis MM, Boniface JJ, Reich Z, Lyons D, Hampl J, Arden B, Chien Y. Ligand recognition by alpha beta T cell receptors. Annu Rev Immunol. 1998;16:523–544. doi:10.1146/annurev.immunol.16.1.523.

9. Fontenot JD, Gavin MA, Rudensky AY. Foxp3 programs the development and function of CD4+CD25+ regulatory T cells. Nat Immunol. 2003;4:330–336. doi:10.1038/ni904.

10. Ivanov II, McKenzie BS, Zhou L, Tadokoro CE, Lepelley A, Lafaille JJ, Cua DJ, Littman DR. The orphan nuclear receptor RORgammat directs the differentiation program of proinflammatory IL-17+ T helper cells. Cell. 2006;126:1121–1133. doi:10.1016/j.cell.2006.07.035.

11. Szabo SJ, Kim ST, Costa GL, Zhang X, Fathman CG, Glimcher LH. A novel transcription factor, T-bet, directs Th1 lineage commitment. Cell. 2000;100:655–669.

12. Zheng W, Flavell RA. The transcription factor GATA-3 is necessary and sufficient for Th2 cytokine gene expression in CD4 T cells. Cell. 1997;89:587–596.

13. Giannakis M, Mu XJ, Shukla SA, Qian ZR, Cohen O, Nishihara R, Bahl S, Cao Y, Amin-Mansour A, Yamauchi M, et al. Genomic correlates of immune-cell infiltrates in colorectal carcinoma. Cell Rep. 2016;15:857–865. doi:10.1016/j.celrep.2016.03.075.

14. Maby P, Galon J, Latouche JB. Frameshift mutations, neoantigens and tumor-specific CD8(+) T cells in microsatellite unstable colorectal cancers. Oncoimmunology. 2016;5:e1115943. doi:10.1080/2162402X.2015.1115943.

15. Gros A, Parkhurst MR, Tran E, Pasetto A, Robbins PF, Ilyas S, Prickett TD, Gartner JJ, Crystal JS, Roberts IM, et al. Prospective identification of neoantigen-specific lymphocytes in the peripheral blood of melanoma patients. Nat Med. 2016;22:433–438. doi:10.1038/nm.4051.

16. Gee MH, Han A, Lofgren SM, Beausang JF, Mendoza JL, Birnbaum ME, Bethune MT, Fischer S, Yang X, Gomez-Eerland R, et al. Antigen identification for Orphan T Cell receptors expressed on Tumor-Infiltrating Lymphocytes. Cell. 2018;172:549–63 e16. doi:10.1016/j.cell.2017.11.043.

17. Wu X, Zhang H, Xing Q, Cui J, Li J, Li Y, Tan Y, Wang S. PD-1 (+) CD8(+) T cells are exhausted in tumours and functional in draining lymph nodes of colorectal cancer patients. Br J Cancer. 2014;111:1391–1399. doi:10.1038/bjc.2014.416.

18. Brahmer JR, Tykodi SS, Chow LQ, Hwu WJ, Topalian SL, Hwu P, Drake CG, Camacho LH, Kauh J, Odunsi K, et al. Safety and activity of anti-PD-L1 antibody in patients with advanced cancer. N Engl J Med. 2012;366:2455–2465. doi:10.1056/NEJMoa1200694.

19. Topalian SL, Hodi FS, Brahmer JR, Gettinger SN, Smith DC, McDermott DF, Powderly JD, Carvajal RD, Sosman JA, Atkins MB, et al. Safety, activity, and immune correlates of anti-PD-1 antibody in cancer. N Engl J Med. 2012;366:2443–2454. doi:10.1056/NEJMoa1200690.

20. Holch JW, Ricard I, Stintzing S, Modest DP, Heinemann V. The relevance of primary tumour location in patients with metastatic colorectal cancer: A meta-analysis of first-line clinical trials. Eur J Cancer. 2017;70:87–98. doi:10.1016/j.ejca.2016.10.007.

21. Missiaglia E, Jacobs B, D'Ario G, Di Narzo AF, Soneson C, Budinska E, Popovici V, Vecchione L, Gerster S, Yan P, et al. Distal and proximal colon cancers differ in terms of molecular, pathological, and clinical features. Ann Oncol. 2014;25:1995–2001. doi:10.1093/annonc/mdu275.

22. Han A, Glanville J, Hansmann L, Davis MM. Linking T-cell receptor sequence to functional phenotype at the single-cell level. Nat Biotechnol. 2014;32:684–692. doi:10.1038/nbt.2938.

23. Hansmann L, Han A, Penter L, Liedtke M, Davis MM. Clonal expansion and interrelatedness of distinct B-Lineage

compartments in multiple Myeloma Bone Marrow. Cancer Immunol Res. 2017;5:744–754. doi:10.1158/2326-6066.CIR-17-0012.

24. Penter L, Dietze K, Bullinger L, Westermann J, Rahn HP, Hansmann L. FACS single cell index sorting is highly reliable and determines immune phenotypes of clonally expanded T cells. Eur J Immunol. 2018;48:1248–1250. doi:10.1002/eji.201847507.

25. Ritter J, Seitz V, Balzer H, Gary R, Lenze D, Moi S, Pasemann S, Seegebarth A, Wurdack M, Hennig S, et al. Donor CD4 T Cell diversity determines virus reactivation in patients after HLA-matched Allogeneic Stem Cell transplantation. Am J Transplant. 2015;15:2170–2179. doi:10.1111/ajt.13241.

26. Siewert K, Malotka J, Kawakami N, Wekerle H, Hohlfeld R, Dornmair K. Unbiased identification of target antigens of CD8+ T cells with combinatorial libraries coding for short peptides. Nat Med. 2012;18:824–828. doi:10.1038/nm.2720.

27. Tran E, Robbins PF, Lu YC, Prickett TD, Gartner JJ, Jia L, Pasetto A, Zheng Z, Ray S, Groh EM, et al. T-Cell transfer therapy targeting mutant KRAS in cancer. N Engl J Med. 2016;375:2255–2262. doi:10.1056/NEJMoa1609279.

28. Friese MA, Jakobsen KB, Friis L, Etzensperger R, Craner MJ, McMahon RM, Jensen LT, Huygelen V, Jones EY, Bell JI, et al. Opposing effects of HLA class I molecules in tuning autoreactive CD8+ T cells in multiple sclerosis. Nat Med. 2008;14:1227–1235. doi:10.1038/nm.1881.

29. Zhang L, Yu X, Zheng L, Zhang Y, Li Y, Fang Q, Gao R, Kang B, Zhang Q, Huang JY, et al. Lineage tracking reveals dynamic relationships of T cells in colorectal cancer. Nature. 2018. doi:10.1038/s41586-018-0694-x.

30. Sasidharan Nair V, Toor SM, Taha RZ, Shaath H, Elkord E. DNA methylation and repressive histones in the promoters of PD-1, CTLA-4, TIM-3, LAG-3, TIGIT, PD-L1, and galectin-9 genes in human colorectal cancer. Clin Epigenetics. 2018;10:104. doi:10.1186/s13148-018-0539-3.

31. Le DT, Uram JN, Wang H, Bartlett BR, Kemberling H, Eyring AD, Skora AD, Luber BS, Azad NS, Laheru D, et al. PD-1 Blockade in tumors with mismatch-repair deficiency. N Engl J Med. 2015;372:2509–2520. doi:10.1056/NEJMoa1500596.

32. Haymaker CL, Wu RC, Ritthipichai K, Bernatchez C, Forget MA, Chen JQ, Liu H, Wang E, Marincola F, Hwu P, et al. BTLA marks a less-differentiated tumor-infiltrating lymphocyte subset in melanoma with enhanced survival properties. Oncoimmunology. 2015;4:e1014246. doi:10.1080/2162402X.2015.1008371.

33. Lan X, Li S, Gao H, Nanding A, Quan L, Yang C, Ding S, Xue Y. Increased BTLA and HVEM in gastric cancer are associated with progression and poor prognosis. Onco Targets Ther. 2017;10:919–926. doi:10.2147/OTT.S128825.

34. Oguro S, Ino Y, Shimada K, Hatanaka Y, Matsuno Y, Esaki M, Nara S, Kishi Y, Kosuge T, Hiraoka N. Clinical significance of tumor-infiltrating immune cells focusing on BTLA and Cbl-b in patients with gallbladder cancer. Cancer Sci. 2015;106:1750–1760. doi:10.1111/cas.12825.

35. Ritthipichai K, Haymaker CL, Martinez M, Aschenbrenner A, Yi X, Zhang M, Kale C, Vence LM, Roszik J, Hailemichael Y, et al. Multifaceted role of BTLA in the control of CD8(+) T-cell fate after antigen encounter. Clin Cancer Res. 2017;23:6151–6164. doi:10.1158/1078-0432.CCR-16-1217.

36. Derre L, Rivals JP, Jandus C, Pastor S, Rimoldi D, Romero P, Michielin O, Olive D, Speiser DE. BTLA mediates inhibition of human tumor-specific CD8+ T cells that can be partially reversed by vaccination. J Clin Invest. 2010;120:157–167. doi:10.1172/JCI40070.

37. Fourcade J, Sun Z, Pagliano O, Guillaume P, Luescher IF, Sander C, Kirkwood JM, Olive D, Kuchroo V, Zarour HM. CD8 (+) T cells specific for tumor antigens can be rendered dysfunctional by the tumor microenvironment through upregulation of the inhibitory receptors BTLA and PD-1. Cancer Res. 2012;72:887–896. doi:10.1158/0008-5472.CAN-11-2637.

38. Chen L, Diao L, Yang Y, Yi X, Rodriguez BL, Li Y, Villalobos PA, Cascone T, Liu X, Tan L, et al. CD38-Mediated immunosuppression as a mechanism of Tumor cell escape from PD-1/PD-L1

blockade. Cancer Discov. 2018;8:1156–1175. doi:10.1158/2159-8290.CD-17-1033.

39. Frohlich M, Gogishvili T, Langenhorst D, Luhder F, Hunig T. Interrupting CD28 costimulation before antigen rechallenge affects CD8(+) T-cell expansion and effector functions during secondary response in mice. Eur J Immunol. 2016;46:1644–1655. doi:10.1002/eji.201546232.

40. Maecker HT, McCoy JP, Nussenblatt R. Standardizing immuno-phenotyping for the Human Immunology Project. Nat Rev Immunol. 2012;12:191–200. doi:10.1038/nri3158.

41. Zvyagin IV, Pogorelyy MV, Ivanova ME, Komech EA, Shugay M, Bolotin DA, Shelenkov AA, Kurnosov AA, Staroverov DB, Chudakov DM, et al. Distinctive properties of identical twins' TCR repertoires revealed by high-throughput sequencing. Proc Natl Acad Sci U S A. 2014;111:5980–5985. doi:10.1073/pnas.1319389111.

42. Liang X, Weigand LU, Schuster IG, Eppinger E, van der Griendt JC, Schub A, Leisegang M, Sommermeyer D, Anderl F, Han Y, et al. A single TCR alpha-chain with dominant peptide recognition in the allorestricted HER2/neu-specific T cell repertoire. J Immunol. 2010;184:1617–1629. doi:10.4049/jimmunol.0902155.

43. Simoni Y, Becht E, Fehlings M, Loh CY, Koo SL, Teng KWW, Yeong JPS, Nahar R, Zhang T, Kared H, et al. Bystander CD8(+) T cells are abundant and phenotypically distinct in human tumour infiltrates. Nature. 2018;557:575–579. doi:10.1038/s41586-018-0130-2.

44. Scheper W, Kelderman S, Fanchi LF, Linnemann C, Bendle G, de Rooij MAJ, Hirt C, Mezzadra R, Slagter M, Dijkstra K, et al. Low and variable tumor reactivity of the intratumoral TCR repertoire in human cancers. Nat Med. 2019;25:89–94. doi:10.1038/s41591-018-0266-5.

45. Li S, Lefranc MP, Miles JJ, Alamyar E, Giudicelli V, Duroux P, Freeman JD, Corbin VD, Scheerlinck JP, Frohman MA, et al. IMGT/HighV QUEST paradigm for T cell receptor IMGT clonotype diversity and next generation repertoire immunoprofiling. Nat Commun. 2013;4:2333. doi:10.1038/ncomms3333.